Influence of Rossby waves on nutrient dynamics and the plankton community structure in the North Pacific subtropical gyre

Carole M. Sakamoto,[1] David M. Karl,[2] Hans W. Jannasch,[1] Robert R. Bidigare,[2] Ricardo M. Letelier,[3] Peter M. Walz,[1] John P. Ryan,[1] Paulo S. Polito,[4] and Kenneth S. Johnson[1]

Received 21 May 2003; revised 29 March 2004; accepted 7 April 2004; published 28 May 2004.

[1] Nitrate concentrations, chlorophyll *a* (Chl *a*) fluorescence, radiance, salinity, and temperature were measured on the Hawaii Air-Sea Logging Experiment, A Long-Term Oligotrophic Habitat Assessment (HALE ALOHA) mooring located near the Hawaii Ocean Time-Series (HOT) Program's Station ALOHA (22°45′N; 158°W). Nitrate concentrations were determined with OsmoAnalyzers deployed at depths of 120 and 180 m. Deployments in 1997 and 1999 captured monthlong events that brought relatively cold high-nitrate seawater up into the euphotic zone. These events were correlated with negative sea surface height (SSH) anomalies measured by the TOPEX/Poseidon satellite altimeter. These nutrient injections at the Hawaii site were predominantly associated with first baroclinic mode Rossby waves. Elevated nitrate concentrations resulted in increased Chl *a* concentrations, increased primary productivity, and shifts in the phytoplankton community structure, as determined by HPLC analysis of pigment concentrations. The relative increase in pigments associated with phytoplankton that can grow rapidly and exploit nitrate (e.g., haptophytes and pelagophytes) coincided with the passage of Rossby waves in 1997–1999. A long-term combination of satellite remote sensing, moored instrumentation or remote vehicles and periodic ship-based sampling is needed to fully characterize the spatial and temporal variability due to the passage of Rossby waves and their associated biological responses. *INDEX TERMS:* 4556 Oceanography: Physical: Sea level variations; 4572 Oceanography: Physical: Upper ocean processes; 4845 Oceanography: Biological and Chemical: Nutrients and nutrient cycling; 4815 Oceanography: Biological and Chemical: Ecosystems, structure and dynamics; 4894 Oceanography: Biological and Chemical: Instruments and techniques; *KEYWORDS:* nitrate, mooring, Rossby waves, phytoplankton, nutrient

Citation: Sakamoto, C. M., D. M. Karl, H. W. Jannasch, R. R. Bidigare, R. M. Letelier, P. M. Walz, J. P. Ryan, P. S. Polito, and K. S. Johnson (2004), Influence of Rossby waves on nutrient dynamics and the plankton community structure in the North Pacific subtropical gyre, *J. Geophys. Res.*, *109*, C05032, doi:10.1029/2003JC001976.

1. Introduction

[2] Imbalances between nitrate inputs and outputs within the euphotic zone of the open ocean are often observed [*Lewis et al.*, 1986; *Planas et al.*, 1999]. For example, *Planas et al.* [1999] found that the average integrated nitrate uptake rate in the central Atlantic exceeded by a factor of two the estimated diffusive nitrate supply. Furthermore, the nitrate uptake exceeded the diffusive supply by nearly three orders of magnitude at the most oligotrophic areas examined. Observations like these have led to alternate hypotheses for physical and biological mechanisms to deliver nutrients into the surface waters. Transport mechanisms such as atmospheric deposition [*Prospero and Savoie*, 1989; *Arimoto et al.*, 1996; *Michaels et al.*, 1996; *Sun et al.*, 2001], vertical circulations at fronts [*Mahadevan and Archer*, 2000; *Martin et al.*, 2001], eddy pumping [*Falkowski et al.*, 1991; *McGillicuddy and Robinson*, 1997; *McGillicuddy et al.*, 1998, 1999; *Siegel et al.*, 1999; *McNeil et al.*, 1999; *Garçon et al.*, 2001], and thermocline uplift by 1000 km scale propagating planetary waves (Rossby waves) [*Cipollini et al.*, 2001; *Uz et al.*, 2001; *Siegel*, 2001; *Wilson and Adamec*, 2002] may cause episodic injections of nutrients into the euphotic zone. Atmospheric deposition appears to be more significant near ocean margins and is not further considered for the subtropical North Pacific ocean budget. Nitrogen fixation may also be more important than previously thought in supplying nitrogen for new production [*Karl et al.*, 1997; *Zehr et al.*, 2001; *Karl et al.*, 2002b], but eventually P, Fe and other essential nutrients must be supplied from allochthonous sources. Buoyancy and vertical migration

[1]Monterey Bay Aquarium Research Institute, Moss Landing, California, USA.
[2]Department of Oceanography, University of Hawaii, Honolulu, Hawaii, USA.
[3]College of Oceanic and Atmospheric Sciences, Oregon State University, Corvallis, Oregon, USA.
[4]Instituto Nacional de Pesquisas Espaciais, São José dos Campos, São Paulo, Brazil.

Copyright 2004 by the American Geophysical Union.
0148-0227/04/2003JC001976$09.00

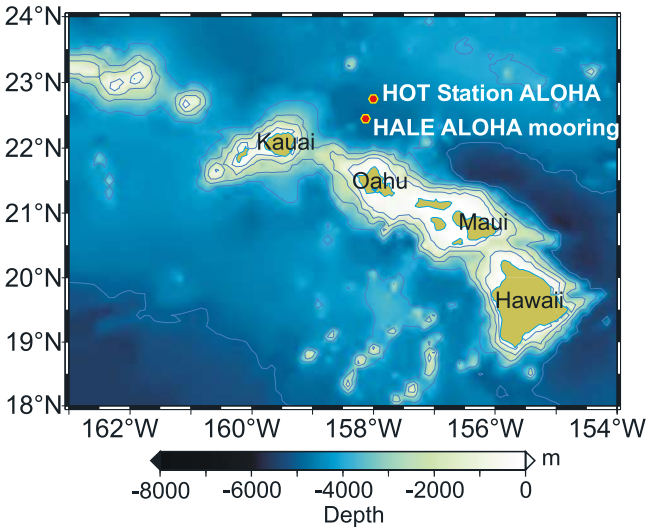


Figure 1. Map of the HOT Station ALOHA location (22°45′N, 158°00′W) and the HALE ALOHA mooring site (22°27′N, 158°8′W) in relation to the Hawaiian Islands. Station ALOHA is approximately 100 km north of Oahu, Hawaii.

of diatoms and *Trichodesmium* might be important but quantitative data are lacking [*Karl et al.*, 1992; *Villareal and Carpenter*, 2003].

[3] The effects of eddy pumping on nitrate transport in the Sargasso Sea was demonstrated with continuous nitrate measurements at the Bermuda Atlantic Time-Series Study (BATS) mooring site in the Sargasso Sea [*McGillicuddy et al.*, 1998; *McNeil et al.*, 1999]. *Siegel et al.* [1999] estimated that mesoscale eddy pumping associated with the first baroclinic mode of motion is a dominant physical mechanism transporting nutrients into the euphotic zone of the Sargasso Sea during the summer and may supply an amount of nutrients that is roughly equal to the nutrients brought up during wintertime convection.

[4] Recently, the potential for planetary or Rossby waves to be an important physical mechanism for uplifting nutrients into the photic zone has been prompted by spectral analysis of the coherence between satellite-derived chlorophyll *a* (Chl *a*) and sea surface height (SSH) data [*Cipollini et al.*, 2001; *Uz et al.*, 2001; *Wilson and Adamec*, 2002]. These large-scale westward propagating waves (a few hundred to several thousand kilometers across) create vertical displacements of the thermocline and SSH anomalies which can be detected by satellite altimetry. The variations in SSH and thermocline depth are associated with increases in Chl *a* concentrations as measured by ocean color, correlating most strongly at latitudes lower than 35°–40° [*Cipollini et al.*, 2001; *Uz et al.*, 2001; *Wilson and Adamec*, 2002].

[5] Since October 1988, the interdisciplinary ocean time series program off Hawaii (Hawaii Ocean Time-Series or HOT) has collected a comprehensive suite of ocean measurements at the oligotrophic Station ALOHA (22°45′N, 158°00′W) in the North Pacific subtropical gyre (Figure 1) [*Karl and Lukas*, 1996]. The approximately monthly shipboard sampling program has enabled collection of an extensive suite of interdisciplinary variables at this site. These observations have provided new insights into fundamental shifts from N limitation to P limitation [*Karl et al.*, 1995; *Karl and Tien*, 1997] and changes in microbial community structure [*Karl*, 1999; *Karl et al.*, 2001].

[6] Although phenomena such as mesoscale eddies and mixed layer deepening events are likely to be important in balancing chemical budgets and establishing community structure, these events are poorly resolved by the traditional expeditionary design of past field programs and even, perhaps, by the approximately monthly HOT sampling design [*Karl et al.*, 2003b]. Thus, to help resolve temporally variable events, a physical-biogeochemical mooring called the Hawaii Air-Sea Logging Experiment, A Long-Term Oligotrophic Habitat Assessment (HALE ALOHA; "hale" is also the Hawaiian word for home) was deployed in January 1997, 30 km south of Station ALOHA. To assess the role of nitrate variations on ecosystem properties, we deployed two in situ osmotically pumped nitrate analyzers (OsmoAnalyzer) on the mooring. One instrument was placed at 120 m and the other at 180 m depth. The sensors logged measurements of nitrate concentrations every ten or fifteen minutes and also recorded temperature and conductivity.

[7] The HALE ALOHA mooring was first deployed in January 1997 and a significant nutrient injection was observed in April that correlated with a physiological response of the phytoplankton community to the changing habitat conditions [*Letelier et al.*, 2000] as well as large increases in net biological oxygen production measured from oxygen saturation and total gas pressure measurements [*Emerson et al.*, 2002]. We report here the changes in nitrate observed during the 1997 event and one observed on a later mooring deployment in 1999. The subsequent biological response is also assessed.

2. Methods

2.1. Nitrate OsmoAnalyzers

[8] Nitrate concentrations were measured with osmotically pumped OsmoAnalyzers [*Jannasch et al.*, 1994]. Although the instrument measures the combination of nitrate and nitrite, we will refer to the resultant species as nitrate in the rest of the paper as it is the dominant species at the HOT site [*Dore and Karl*, 1996]. The chemistry is based on the standard colorimetric method in which the sample stream is combined with an imidazole buffer and the nitrate is reduced to nitrite by passing over a copperized cadmium catalytic surface. The nitrite then reacts with p-aminobenezenesulfonamide (sulfanilamide) and N-1-naphthylethylenediamine dihydrochloride (NED) in an acidic medium to produce an azo dye. Light transmittance through the azo dye solution is measured at 560 nm with a simple LED/photodiode detector [*Betteridge et al.*, 1978]. Seawater nitrate standards and deionized water blanks were injected every four days into the sample manifold with modified solenoid pumps (The Lee Company, PN#LPLX0501-350). Details of the osmotic pumps, chemistry, manifold, electronics, and testing were previously published [*Jannasch et al.*, 1994]. Modifications include a 0.5 mm flow path milled directly into a flat sheet of rigid PVC fitted with a solid disk of cadmium (2 mm thick by 10 mm diameter) and a small

amount of copper is added to the imidazole buffer (0.002 M $CuSO_4$) to extend the usable lifetime of the cadmium reduction surface.

[9] Temperature and conductivity were measured with C-T sensors (Falmouth Scientific, Inc.). WETStar fluorometers (Wet Labs) were also occasionally deployed. Richard Brancker Research (RBR) XX-105 ocean temperature data loggers were deployed at depths of approximately 2, 40, 50, 60, 80, 90, 100, 110, 120, 130 and 150 m [*Letelier et al.*, 2000]. Monthly ship-based sampling at HALE ALOHA was also conducted during the regularly scheduled HOT cruises.

2.2. TOPEX/Poseidon Sea Surface Height Anomaly Data

[10] In 1992, the TOPEX/Poseidon (T/P) satellite altimeter began to provide accurate measurements of global SSH. Variations in the SSH are due to either a net flux of mass or variations in the depth-averaged density of the water column [*Polito and Liu*, 2003]. In the tropics, the SSH anomalies are primarily forced through changes in the upper layer temperature profile [*Chambers et al.*, 1997]. We used two sets of T/P data obtained from the Physical Oceanography Distributed Active Archive Center at the NASA Jet Propulsion Laboratory (JPL) (http://seablade.jpl.nasa.gov/gui) in this paper. To compare SSH anomalies with time series of measurements at the mooring, we used 6-km along-track T/P SSH data from the 4 points nearest the mooring. These points, spanning 18 km along-track were ~20 km from the mooring location and were averaged to form the local SSH anomaly time series. The bounding coordinates for the HALE ALOHA location were (22.61–22.81°N, 157.76–157.86°W) and for Station ALOHA were (22.30–22.50°N, 157.90–158.00°W).

[11] To examine Rossby wave variability using SSH data, the T/P data must be in a 2-D zonal/temporal grid in order to infer the zonal phase speed which is essential to identifying propagating signals. T/P data obtained from JPL originally bin-averaged 0.5° × 0.5° × 10 days (approximately one T/P repeat cycle) were interpolated to 1° × 1° × 10 days using a continuous curvature gridding algorithm [*Polito et al.*, 2000] in the Pacific between 180° to 140°W. The SSH anomaly data were decomposed with a series of 2-D finite impulse response (FIR) band-pass filters into a basin-scale nonpropagating signal (mostly due to seasonal heating, ENSO, cooling, and large-scale advective effects) and westward propagating anomalies interpreted as Rossby wave signals [*Polito et al.*, 2000; *Polito and Liu*, 2003]. Rossby wave activity in the region of HALE ALOHA was examined using the FIR results from 22.5°N.

3. Results

3.1. Nitrate Measurements

[12] The HALE ALOHA mooring was deployed 8 times during the period from January 1997 to June 2000; a total of 16 nitrate OsmoAnalyzers were deployed during the duration of the HALE ALOHA experiment. The nitrate Osmo Analyzer deployed at 180 m was near the base of the nitracline, while the instrument deployed at 120 m was near the depth of the Chl *a* maximum [*Karl et al.*, 2001]. Three instruments were lost due to two mooring failures and two instruments were lost due to pressure housing failures.

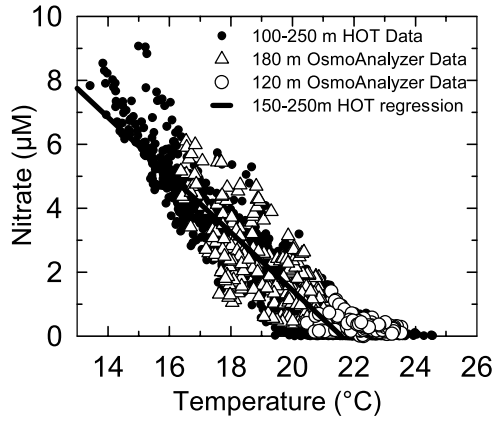


Figure 2. Daily averaged nitrate versus temperature data from the 120 m (open circle) and 180 m (open triangle) OsmoAnalyzer deployments overlain on the HOT Station ALOHA time series discrete samples (filled circles) from the 100–250 m depth range for years 1988–2000. The regression line calculated from the discrete samples in the depth range 150–250 m is also shown.

Of the remaining deployments, a total of 320 days of usable data was produced by the nitrate OsmoAnalyzer at 180 m depth during 6 deployments. Two deployments of the OsmoAnalyzer at 120 m had electronics failures, which leaves three remaining deployments that produced a total of 134 days of usable data. The maximum expected endurance of the OsmoAnalyzer in 20°C seawater is approximately 100 days after which time all of the reagents are consumed. On the basis of a 100 day maximum endurance, the sample return rate was 53% at 180 m and 45% at 120 m depth.

[13] The OsmoAnalyzer was programmed to calibrate itself at about four day intervals by injecting seawater nitrate standards and deionized water blank solutions. The blank and standard pumps did not always operate consistently, so the calibration was augmented with the discrete samples collected on the approximately monthly HOT sampling cruises. The temperature, salinity, and fluorometer measurements were also calibrated with discrete measurements collected at the HALE ALOHA mooring site.

[14] The daily averaged nitrate versus temperature data from the 120 and 180 m OsmoAnalyzer deployments are shown in Figure 2. Superimposed on the plot are the HOT Station ALOHA discrete sample data from the 100–250 m depth range for years 1988–2000. The OsmoAnalyzer temperature and nitrate data were binned into daily averages to reduce tidal signals and differences in the response rate of the two sensors. The OsmoAnalyzer nitrate data fall within the range measured at Station ALOHA. To some extent the agreement is forced at the points that used the HOT discrete data to calibrate the measurements, but the variance of both data sets is similar.

3.2. The Physical Environment

[15] Figure 3a shows the time series of temperature measured on the mooring from 1997–1999 with temperature loggers at depths from 2 to 150 m. Two different processes can be discerned from this plot. The effects of seasonal warming of the upper waters during each summer

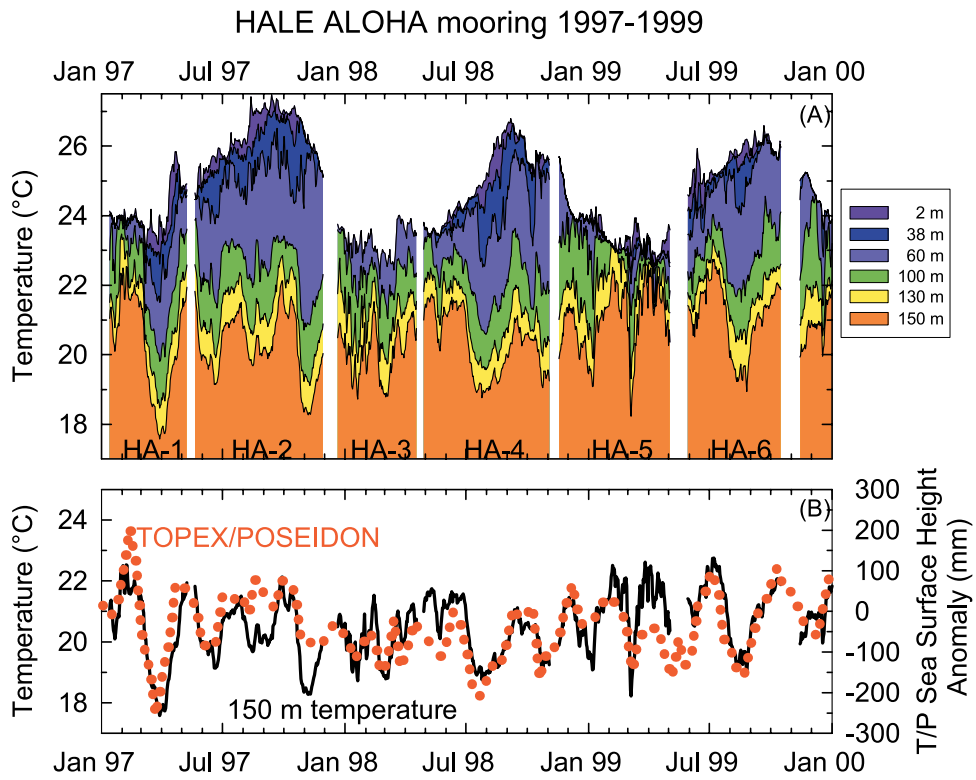


Figure 3. (a) Time series of temperature from 1997–1999 measured with thermistors at depths from 2 to 150 m on the HALE ALOHA mooring. (b) The 150 m temperature data (solid line) and the TOPEX/Poseidon (T/P) sea surface height (SSH) anomaly (mm) (dotted line). The T/P SSH anomalies (mm) are calculated as the differences from the 4-year mean (1993–1996). The four closest T/P data points that average a 6 km^2 area with bounding coordinates of 22.30–22.50°N and 157.90–158.0024°W were downloaded from the NASA Jet Propulsion Laboratory (http://oceanesip.jpl.nasa.gov/gui) using the 6-km along track data set. This 10-day data set was then linearly interpolated to generate a 5-day data set for plotting purposes.

and fall are apparent each year. The temperature data during 1997–1998 also show the large warming associated with El Niño. Decoupled from the upper water column seasonal warming are periodic excursions toward cooler temperatures in the deep waters (>100 m). The T/P SSH anomaly at Station ALOHA is shown in Figure 3b along with the temperature at 150 m. The large temperature excursions at 150 m are coincident with the 'dips' in the T/P SSH anomalies (Figure 3b). These large decreases in SSH and temperature could be due to a variety of physical processes, including cold core eddies passing the mooring site [*Letelier et al.*, 2000] or Rossby waves [*Uz et al.*, 2001; *Polito et al.*, 2000]. Continuous records of nitrate concentrations were collected in two of the largest events during the HALE ALOHA 1 (HA-1) deployment in spring 1997 and the HALE ALOHA 6 (HA-6) deployment in late summer of 1999.

3.3. The HALE ALOHA 1 Deployment

[16] The daily average concentration of nitrate, Chl *a* [*Letelier et al.*, 2000], temperature, and SSH anomaly from the HA-1 mooring deployment in 1997 are shown in Figure 4. Note the inverted scales for the SSH anomaly and temperature data. The nitrate (filled circles) and Chl *a* (filled triangles) data from the Station ALOHA time series study are also shown.

[17] The mooring observations clearly show the correlation of the sea surface depression with the shoaling of the nitracline. The sensor at 180 m is near the base of the euphotic zone [*Karl et al.*, 2001; *Letelier et al.*, 2004]. This event caused a significant nitrate increase in the photic zone. The average and standard deviation of the nitrate concentration at 180 ± 5 m depth at Station ALOHA for years 1988–1999 is 1.96 ± 1.09 μmol/kg (n = 102). The daily average nitrate concentrations at the same depth increase almost threefold at the peak of the sea surface depression (24 March to 1 April) to 5.48 ± 0.54 μmol/kg (n = 9). Temperatures at 180 m also drop from ~20°C to below 17°C during this event.

[18] *Letelier et al.* [2000] examined this event in detail and Chl *a* and Chl *a* fluorescence efficiency (CFE) values that were derived from their spectroradiometer deployed at 25 m depth are also shown in Figure 4 (bottom panel). As the SSH began to drop in late February-early March, the temperature measured at 180 m began to decrease and nitrate concentrations at 180 m and CFE started to increase. Significant increases in the concentration of Chl *a* in the upper 25 m of the water column were measured between 21 March and 10 April, lagging the increases in nitrate measured at 180 m (first observed on 2 March). The mean Chl *a* concentration reached 0.26 μg/L on 30 March corresponding to a threefold increase compared to the mean of 0.07 μg/L recorded

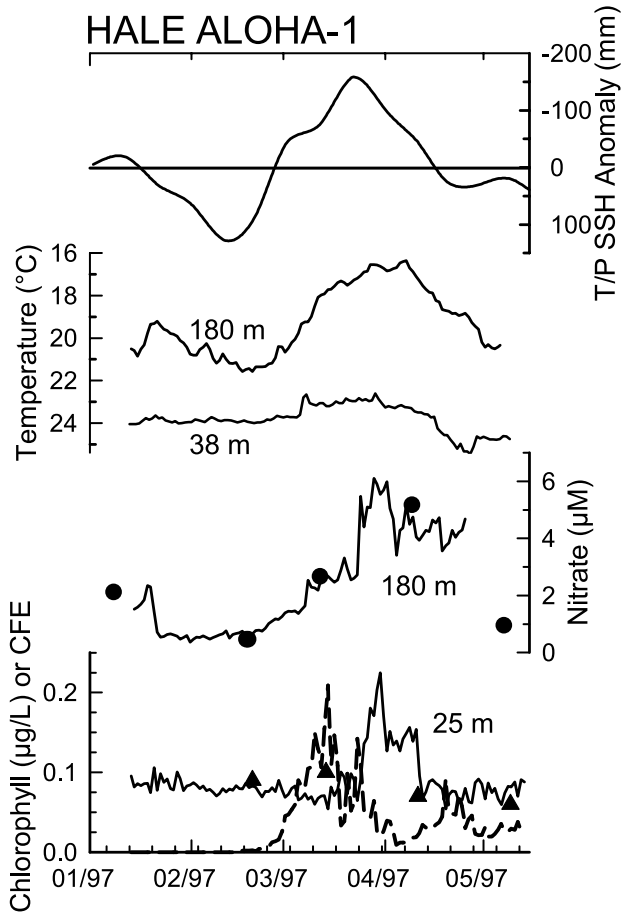


Figure 4. Multipanel plot of the HALE ALOHA-1 deployment with the SSH anomaly measured by the T/P satellite in the top panel followed by temperature at 180 and 38 m, OsmoAnalyzer nitrate concentrations at 180 m, and Chl *a* concentrations (black line) and the Chl *a* fluorescence efficiency (short dash) at 25 m [*Letelier et al.*, 2000] in the bottom panel. The HOT Station ALOHA discrete nitrate (filled circles) for 180 m and discrete Chl *a* (filled triangles) collected at the mooring site are also shown. The temperature, OsmoAnalyzer nitrate, and Chl *a* data (lines) are binned into daily averages to reduce tidal signals and differences in the response rate of the chemical and physical sensors.

between 16 January and 20 March and the mean of 0.08 μg/L over the first 9 years of the HOT field program [*Letelier et al.*, 2000]. Although the time series station sampling captured the initial rise in nitrate, the highest nitrate and Chl *a* concentrations were missed by a few days.

[19] Chlorophyll *a* concentrations at 25 m began decreasing on 11 April although nitrate concentrations remained elevated at 180 m. Discrete nitrate concentrations measured at the HALE ALOHA station conducted on 11 April were below the detection limit of 2 nmol/kg in the upper 75 m and increased to 2.6 μmol/kg at 100 m depth. Synoptic sea surface temperature data from the Advanced Very High Resolution Radiometer (AVHRR) satellite sensor (not shown) indicate that a relatively warm filament coming from the south may have entered the mooring site in mid-April when the 25 m Chl *a* dropped sharply but nitrate remained elevated at 180 m despite the SSH anomaly becoming positive. The secondary peak in the CFE in the latter part of April could signal the depletion of nutrients in the surface waters [*Letelier et al.*, 2000] associated with this filament.

3.4. The HALE ALOHA 6 Deployment

[20] Another event was observed in August 1999 during the sixth HALE ALOHA deployment. The daily averaged values of nitrate (180 m) and temperature (110 and 180 m) are shown in Figure 5. Note again the inverted scales for the T/P SSH anomaly shown in the top panel and the temperature data. Daily averaged data from a WETStar fluorometer (Wet Labs) deployed with a Model SBE-16 SeaBird CTD (SeaBird Electronics) at 110 m are also shown. This fluorometer is located near the deep Chl *a* maximum at 125 m.

[21] The SSH anomaly (note scale reversal) started becoming negative around 11 July. The temperature at 180 m started dropping on 22 July and nitrate concentrations began increasing dramatically on 29 July. The Chl *a* concentration, as estimated by the fluorometer at 110 m, started increasing

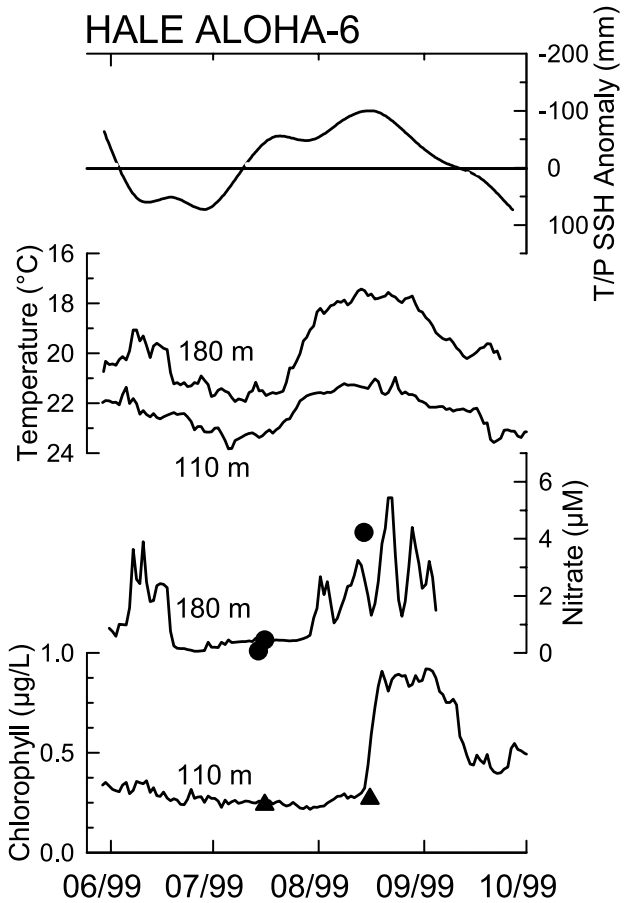


Figure 5. Multipanel plot of the HALE ALOHA-6 deployment with the SSH anomalies measured by the T/P satellite in the top panel followed by temperature at 180 and 110 m, OsmoAnalyzer nitrate concentrations at 180 m, and Chl *a* concentration at 110 m in the bottom panel. The HOT Station ALOHA discrete nitrate (filled circles) at 180 m and the discrete Chl *a* (filled triangles) concentrations sampled at the mooring site for the sixth mooring deployment are also shown. The OsmoAnalyzer nitrate, temperature, and Chl *a* data have been binned into daily averages.

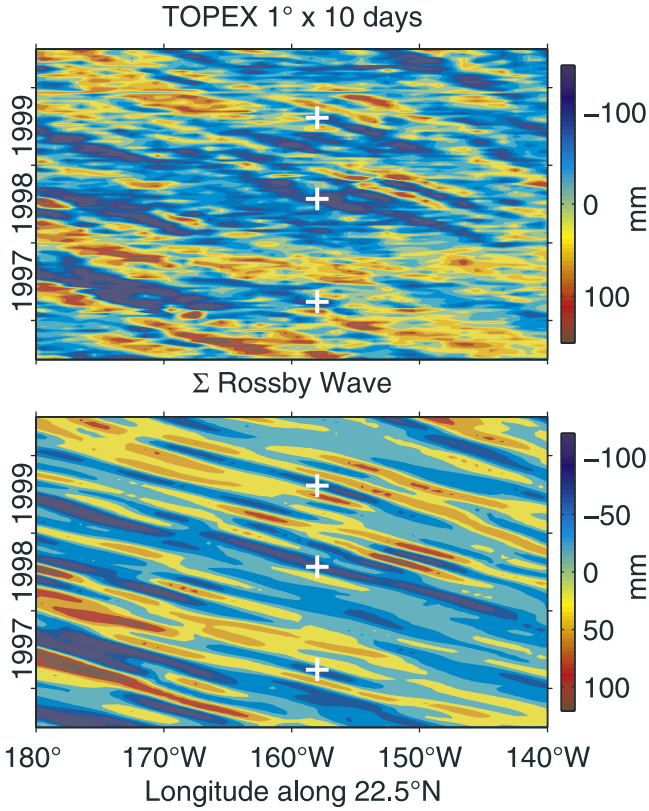


Figure 6. Longitude-time diagrams (Hovmöller plot) of the T/P SSH anomalies along 22.5°N from June 1996 to June 2000. The top panel shows the SSH anomalies, and the lower panel shows the sum of the Rossby wave components. The time periods of the three largest negative sea level anomalies at HOT (centered on 3/29/1997, 7/26/1998, and 8/11/1999) are plotted as white crosses.

slowly around 3 August and then began increasing rapidly around 14 August. The lag in biological response at 110 m is not due to a lag in cold water reaching that depth as the temperature at 110 m depth had started decreasing coincident with the 180 m temperature. Chlorophyll *a* concentrations reached a peak 5 days later on 19 August and then started to decline 17 days later around 5 September. The HOT monthly cruise sampled Station ALOHA during the 12–15 August time period and sampled at the HALE ALOHA site on 16 August. Although the shipboard sampling captured the high-nitrate concentrations associated with the shoaling of isotherms, the peak in the Chl *a* concentration, which was more than 2.5 times the average concentration, was missed by a few days. Similar to the April 1997 event, significant increases in Chl *a* concentrations lagged the nitrate increase by about two weeks. The nitrate OsmoAnalyzer exhausted its reagent supply on 5 September and the nitrate concentration during bloom termination was not observed.

4. Discussion

4.1. Physical Forcing: Influence of Rossby Waves

[22] It is clear from the HALE ALOHA-1 (Figure 4) and HALE ALOHA-6 (Figure 5) deployments that there is a close coupling between negative SSH anomalies and the upward transport of nitrate. The major question that arises is what causes these changes in SSH at HOT? Appropriately filtered T/P SSH anomaly data can be used to unambiguously detect Rossby waves over the world ocean [*Chelton and Schlax*, 1996]. At Station ALOHA, the spectrum derived from 2-D FIR filtering of the SSH anomaly data is dominated by Rossby waves (accounting for 62% of the variance) and those with a period of approximately 3 months are particularly intense in the northern tropical Pacific in this region [*Polito et al.*, 2000; *Polito and Liu*, 2003]. A Hovmöller diagram at 22.5°N for the unfiltered T/P SSH anomaly data and for the filtered (westward propagating) component is shown in Figure 6.

[23] The time periods of the three largest negative sea level anomalies at HOT are plotted as white crosses on each of the Hovmöller diagrams (Figure 6). These crosses fall in the troughs of SSH anomaly on both the unfiltered and the filtered component plots. The anomalies can be tracked over many tens of degrees of longitude and over many months as they propagate westward at Rossby wave speeds. The spatial scales and periods of Rossby waves at the latitude of Station ALOHA are long compared to the spatial and temporal resolution of the T/P SSH data, which allows Rossby waves to be well resolved. Additionally, the application of the FIR method permitted an accurate estimation of the parameters that characterize the unique dynamical regime of these waves. At the latitude of Station ALOHA, the shortest westward propagating signals identified as long, first mode baroclinic Rossby waves have wavelengths larger than ~600 km and periods of ~90 days [*Polito and Liu*, 2003]. In contrast, mesoscale eddies are difficult to sample and quantify. Because of the gridding and filtering methods, eddies spanning less than 3 degrees of longitude (308 km at the latitude of Station ALOHA) are not adequately quantified by our methods. Using high-resolution altimetric fields from combined T/P and ERS-2 measurements, *Letelier et al.* [2000] describe a cyclonic eddy with a diameter of 100–150 km at Station ALOHA. Because the scale of eddies observed in this region is significantly smaller than the passband of our FIR filter applied to 1 degree gridded T/P fields, we do not attempt to quantify eddy variation by these methods.

[24] The event captured during HALE ALOHA-6 is probably associated with only a Rossby wave as high-resolution sea surface temperature imagery (not shown) confirmed that there was no indication of an eddy around the mooring during this time period. In contrast, the event captured during HALE ALOHA-1 may be associated with both the simultaneous passage of the trough of a Rossby wave and a cyclonic mesoscale eddy (Figure 4). Results from an objective analysis using combined T/P and ERS 2 satellite altimeters [*Letelier et al.*, 2000] indicate the passage of a cyclonic mesoscale eddy during this time period. In addition, high-resolution sea surface temperature imagery (not shown) also indicates that a relatively warm filament coming from the south may have flowed across the mooring site in mid-April. Because each event is clearly associated with the presence of a strong Rossby wave trough, we conclude that these waves can be a mechanism for driving a biological response. In contrast to an eddy that may have persistent isolation of a water mass, the dominant process in a Rossby wave influencing the Chl *a* concentration is the

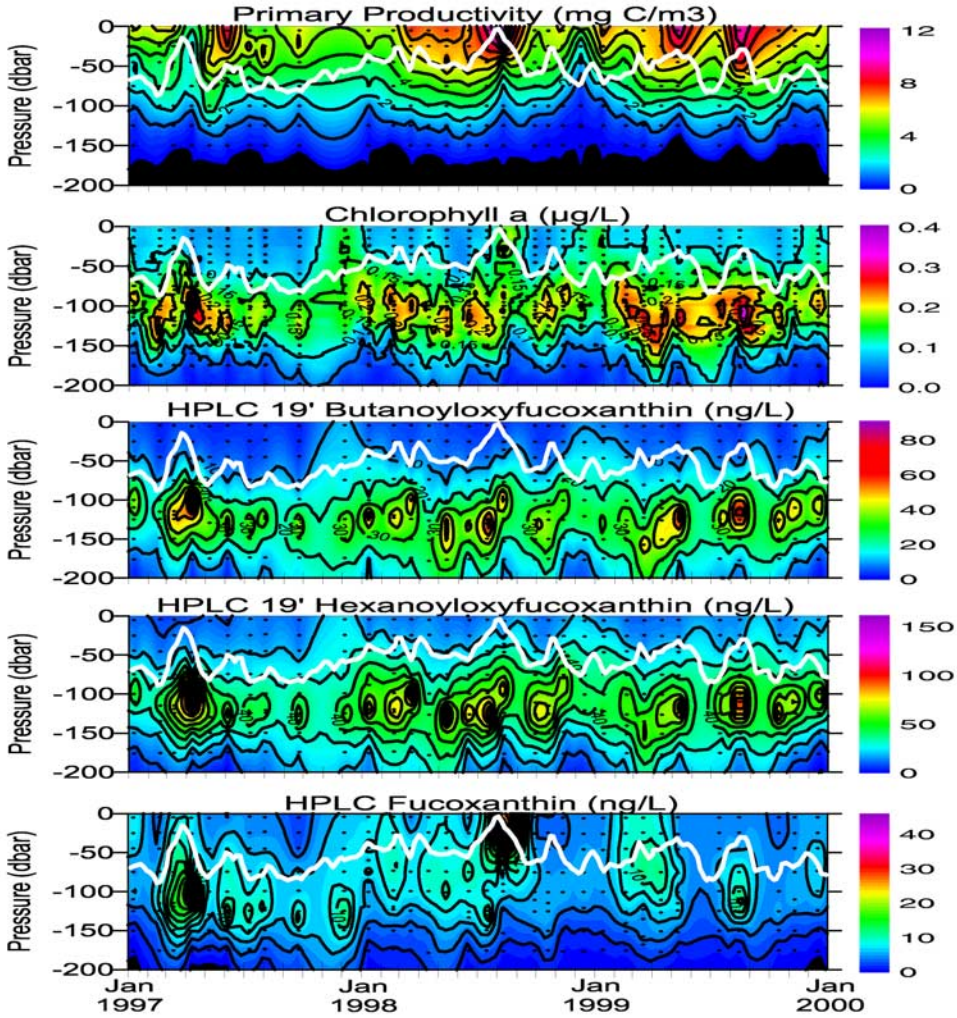


Figure 7. Multipanel plot of the HOT Station ALOHA time series contours of primary productivity, total Chl-*a*, HPLC measured 19′-butanoyloxyfucoxanthin, 19′-hexanoyloxyfucoxanthin, and fucoxanthin for the time period 1997–1999. The T/P SSH anomaly is shown as a white overlay with negative values at the top of the plots.

vertical transport associated with vortex stretching. There is a lag in the mooring data between the nutrient injection associated with the isotherm uplift and the subsequent biological response. This delay may reflect time for phytoplankton growth to occur and the time delay for uplift and diffusion of nutrients into the photic zone. In contrast, the biological, chemical and physical responses to eddies that pass by moorings near Bermuda are nearly simultaneous [*McGillicuddy et al.*, 1998; *McNeil et al.*, 1999] because a well established phytoplankton community is already present in the eddy.

4.2. Biological Response to Nutrient Injections

[25] There are relatively few OsmoAnalyzer deployments where we can demonstrate the nitracline has shoaled. However, the data in Figures 4 and 5 demonstrate that the nitrate concentration increase is closely coupled to the SSH anomaly detected by the T/P satellite altimeter at the HOT site. We have, therefore, used the SSH anomaly as a proxy for nitrate injection into the euphotic zone to estimate the impact of nutrient injection events on biogeochemical processes at the HOT site. Phytoplankton community response to uplift of the nitracline can be determined by correlating measurements made during HOT monthly sampling cruises with the SSH anomaly.

[26] Community biological response to uplifted nitracline levels can be seen in the contour plots of the primary productivity and total Chl *a* for 1997–1999 (Figure 7). The T/P SSH anomaly (note scale is inverted) is superimposed as a white line. Increased primary productivity in the surface waters and increased Chl *a* levels tend to be associated with the nutrient injection events although exceptions occur. Shifts in community structure are apparent during these periods of negative SSH anomalies (shown as peaks in the white lines). The contour plots of the concentration of the pigments 19′-butanoyloxyfucoxanthin, 19′-hexanoyloxyfucoxanthin, and fucoxanthin show increases associated with negative SSH anomalies (Figure 7). These carotenoid pigments are diagnostic markers for pelagophytes, haptophytes, and diatoms, respectively

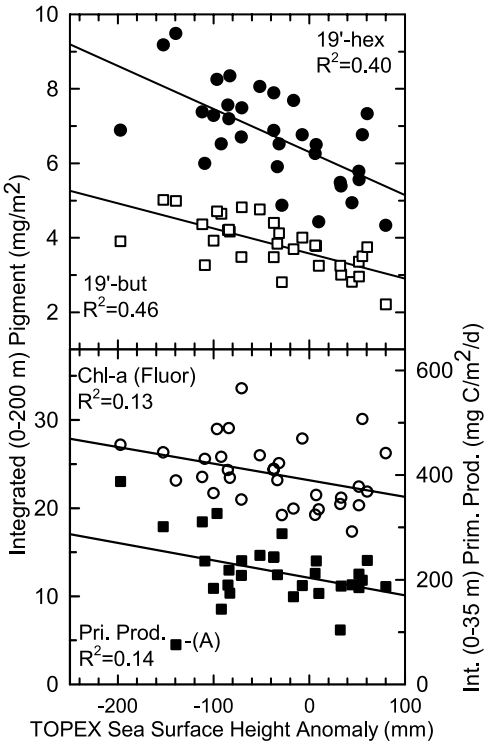


Figure 8. Station ALOHA 0–200 m integrated 19′–hexanoyloxyfucoxanthin (filled circles) and 19′-butanoyloxyfucoxanthin (open squares) in the top panel and Chl *a* by fluorescence (open circles) and primary productivity (filled squares) in the bottom panel versus the T/P SSH anomaly. The SSH data were interpolated to the dates of the HOT cruises. The regression line and coefficient of determination (R^2) are also shown for each parameter. If the primary productivity labeled "A" is eliminated from the regression, the coefficient of determination doubles to 0.31. The coefficient of determination for SSH anomaly versus zeaxanthin is less than 0.01 (not plotted).

[*Andersen et al.*, 1996]. The haptophytes and pelagophytes have been found to be the two most abundant groups of eukaryotes at Station ALOHA [*Andersen et al.*, 1996]. The highest fucoxanthin levels tend to be associated with the strongest Rossby wave signatures.

[27] Regression plots of the 1997–1999 integrated (0–200 m) 19′-hexanoyloxyfucoxanthin, 19′-butanoyloxyfucoxanthin, fluorometric Chl *a*, and primary productivity (0–35 m) versus the T/P SSH anomaly are shown in Figure 8. The integrated 19′-hexanoyloxyfucoxanthin and 19′-butanoyloxyfucoxanthin have significant negative correlations with the SSH anomaly. The highest concentrations of these marker pigments for haptophytes and pelagophytes are associated with negative SSH anomalies. This indicates that as isotherms are uplifted, these phytoplankton respond to the nitrate injections into the euphotic zone. Although the occurrence of negative SSH anomalies and increases in primary productivity can be seen in Figure 7, the coefficient of determination (R^2) of the integrated 0–35 m primary productivity versus SSH is only about 0.1–0.2. The coefficient of determination increases to 0.31 if a single large outlying point, which is labeled (A) in Figure 8, is eliminated. The primary productivity was only integrated from the surface to a depth of 35 m in this analysis because the production of pigments near the surface causes light limitation of phytoplankton in subsurface waters [*Letelier et al.*, 2000]. As a result, primary production tends to decrease below the near surface highs that occur as Rossby waves pass the HOT station (Figure 7). An R^2 value of 0.13 was obtained between the SSH anomaly and integrated Chl *a* concentration.

[28] On the other hand, there does not appear to be a correlation with zeaxanthin and divinyl Chl *a* (not shown) indicating that cyanobacteria are not affected by the nutrient injections. The lack of a SSH anomaly correlation with zeaxanthin ($r^2 < 0.001$, not shown), which is a pigment associated with cyanobacteria, suggests that these phytoplankton are not influenced by nitrate availability. Indeed, cyanobacteria populations are dominated by *Prochlorococcus* at Station ALOHA [*Campbell et al.*, 1994] and recent analysis of the *Prochlorococcus* genome has shown that the organism lacks the genes required for nitrate uptake and reduction and therefore cannot utilize nitrate [*Moore et al.*, 2002].

4.3. Importance of Rossby Waves to Primary Productivity

[29] At Station ALOHA, comparisons of heat storage and SSH anomalies indicate that 62% of the variance is associated with Rossby waves [*Polito et al.*, 2000]. Estimates of the impact of this variability on ecosystem properties during a single large event can be derived from the regression lines in Figure 8 by comparing the expected value at the lowest T/P SSH anomaly (−197 mm) to the expected value at the mean T/P SSH anomaly. The passage of the largest Rossby waves, and possible mesoscale eddies that occur during these events, may drive integrated (0–35 m) primary productivity values up 25% and increase integrated (to 200 m) 19′-hexanoyloxyfucoxanthin and 19′-butanoyloxyfucoxanthin concentrations by 27% and 28%, respectively. Integrated (0–200 m) Chl *a* increases by only 7%.

[30] Thus the strongest events can produce a significant enhancement compared to the mean, but events of this magnitude happen infrequently. The impact of Rossby waves over multiple years on the mean values for ecosystem properties can be estimated by combining a frequency distribution of the T/P SSH anomaly with regression lines in Figure 8. The elevated values associated with the lowest 30% of the SSH anomaly values (SSH anomaly < −50 mm) account for 34% of the total integrated 19′-hexanoyloxyfucoxanthin and 19′-butanoyloxyfucoxanthin concentrations, 32% of the total integrated Chl a concentration, and 33% of the total integrated primary productivity during 1997–1999. The passage of Rossby waves and mesoscale eddies results in enhancement of primary productivity and accumulation of pigments associated with phytoplankton that can exploit the nitrate that is entrained, but the effects may contribute less than around 5–10% enhancement of the mean. This result is not surprising as the slopes of the regression lines in Figure 8 are not very steep. The slopes of the regression lines for 19′-hexanoyloxyfucoxanthin, 19′-butanoyloxyfucoxanthin, and Chl a in Figure 8 could be steeper if the highest concentrations of the pigments were missed due to sampling timing.

[31] Although the enhancement due to these types of events on the total primary productivity is probably less than 5–10% on average, the impact of episodic nutrient injections on carbon export and new primary production may be more significant. Sporadic blooms of large diatom species responding to episodic nutrient injections at the base of the euphotic zone could make a disproportionately large contribution to new primary production that would not be observed with traditional methods for measuring phytoplankton rate processes [*Goldman*, 1993]. *Benitez-Nelson et al.* [2001] used the disequilibrium between particle reactive ^{234}Th and its soluble parent ^{238}U to quantify the net rate of particle export in the upper waters of Station ALOHA. This method integrates the ^{234}Th fluxes over approximately 35 days and the monthly sampling period should capture increased particle export following the passage of a Rossby wave. The October 1999 sampling, following the HA-6 event, did indeed capture a very high ^{234}Th deficit (approximately 4x greater than the mean) over the upper 150 m of the water column. Carbon export was 2 to 3 times greater than the average flux, and may reflect increased particulate export flux at the end of this nutrient injection event. This Th imbalance could have resulted from a summer bloom event associated with high stratification in the water column that are a recurrent phenomenon at Station ALOHA [*Karl et al.*, 1992; *Scharek et al.*, 1999; *Karl et al.*, 2002a, 2003a]. If this is the case, the shoaling of the nutricline associated with the Rossby wave could enhance these blooms. So, although the contribution of these types of events to the overall primary productivity may not be large, the shifts in community structure to phytoplankton species that contribute disproportionately to the export flux may be very significant.

4.4. The Coherence of Satellite-Derived CHL *a* Concentration and Altimeter Measurements

[32] The statistical coherence of Rossby waves with global ocean color at midlatitudes may be consistent with a nutrient injection mechanism. However, other explanations have been proposed [*Uz et al.*, 2001; *Charria et al.*, 2003; *Dandonneau et al.*, 2003]. Two mechanisms generally hypothesized to account for the effect of Rossby waves on surface ocean color are: (1) uplift of the deep Chl *a* maximum layer due to the passage of a Rossby wave which brings more phytoplankton cells closer to the surface, changing the amount of phytoplankton seen by the satellite without changing the vertically integrated amount, or (2) shoaling of the nitracline due to the thermocline fluctuations associated with a Rossby wave and thus there is a direct effect on the growth of nutrient-limited cells resulting from a nutrient injection into the euphotic zone. In addition, it has also been suggested that the ocean color signature results from the accumulation of phytoplankton detritus in convergent zones as the waves pass [*Dandonneau et al.*, 2003].

[33] The first proposed mechanism of isopycnal uplift bringing phytoplankton cells closer to the surface and increasing the Chl *a* concentration that the satellite senses without a change in the vertically averaged amount. The initial uplifting of isopycnals in HALE ALOHA-1 did produce a strong CFE signal measured at 25 m [*Letelier et al.*, 2000, Figure 4]. This suggests that phytoplankton brought into the surface layer did not have time for photoadaptation to the change in light and thus the sudden rise of the thermocline resulted in phytoplankton physiological stress from the increase in photosynthetically available radiation (PAR) exposure [*Letelier et al.*, 2000]. It is conceivable that increases in PAR exposure from the arrival of Rossby waves before increases in nutrient availability (i.e., before the shoaling of the nitracline to the upper euphotic zone) would initially result in an increase in the amount of radiation absorbed by phytoplankton without an increase in carbon fixation and thus the probability of energy dissipation by the phytoplankton as fluorescence and heat increases [*Letelier et al.*, 2000]. Although uplifting of the thermocline would expose phytoplankton to increased PAR levels and could increase their fluorescence, at Station ALOHA the deep Chl *a* maximum occurs at a great enough depth (110–120 m) that it would not be uplifted close enough to the surface to reach the SeaWIFS optical depth zone of 25–40 m to account for the satellite color signals. Everyday at Station ALOHA there are short-term vertical displacements of the thermocline and deep Chl *a* maximum that range from 14–69 m (33 ± 10 m, n = 107) within an inertial period (approximately 31 hours) that are also not seen by satellite remote sensing [*Karl et al.*, 2002a]. Finally, the contour plots of Chl *a* and T/P from 1997–1999 show periods of increased Chl *a* concentrations in the vertical associated with the passage of Rossby waves (Figure 7). The hypothesis that the sea color anomalies are only due to Rossby wave-induced convergences of floating particles on the surface and not from nutrient inputs [*Dandonneau et al.*, 2003] is also not supported by the statistically significant increases in integrated pigment concentrations during sea surface lows (Figure 8).

[34] The second mechanism, nutrient injection, is supported by the correlation between increased concentration of pigments integrated from 0 to 200 m that are associated with nitrate limited species (19′-butanoyloxyfucoxanthin and 19′-hexanoyloxyfucoxanthin) with negative SSH anomalies during 1997–1999. In this scenario, the passage of Rossby waves raises the thermocline and thus the nitracline into the euphotic zone resulting in higher productivity and a shallowing of the deep chlorophyll maximum. There is a lag until the nitracline is displaced upward into the euphotic zone and there is also a physiological lag between the availability of nutrients and increases in growth rate which may result in the low biomass accumulation seen in the leading edge of the Rossby wave which turns into higher biomass (Chl *a* concentrations) in the trailing edge as the water mass subsides.

[35] During this time period, the data indicate that passage of a Rossby wave can uplift nutrients and enhance biological productivity. Several questions remain, however. It is still unclear how nutrients that are injected at the base of the euphotic zone reach the mixed layer, and as *Lewis* [2002] points out, there must be a restoring term that brings the nutrient concentration on the isopycnal surfaces below the euphotic zone back to equilibrium on short enough timescales to prevent the nitracline from getting 'pushed' to a deeper isopycnal surface that would not be brought into the euphotic zone with subsequent events. Three possible mechanisms for restoring the nitrate density relationship

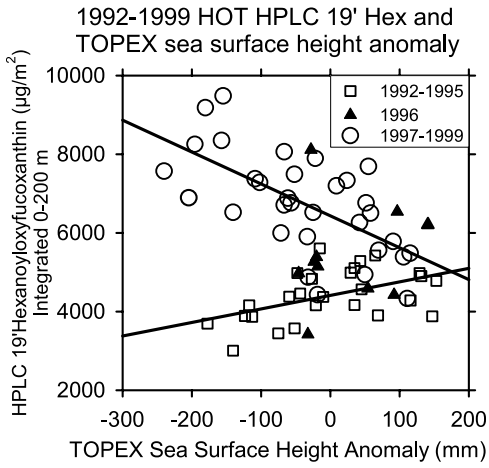


Figure 9. Regression plots of 0–200 m integrated Station ALOHA HPLC 19′-hexanoyloxyfucoxanthin versus TOPEX SSH for the time periods 1992–1995 ($y = 3.438x + 4414$, $r^2 = 0.242$, $n = 26$), 1996 ($y = 2.529x + 5354$, $r^2 = 0.0174$, $n = 10$), and 1997–1999 ($y = -8.107x + 6432$, $r^2 = 0.4021$, $n = 32$). The regression lines for the 1992–1995 and 1997–1999 time periods are plotted as solid lines. The SSH data were interpolated to the dates of the HOT cruises.

following eddy-driven productivity events have been reviewed by *McGillicuddy et al.* [2003] and include remineralization of sinking particulate material from above, isopycnal mixing processes, and diapycnal processes. In contrast to an eddy-driven event where the nutrient injection occurs only once as the eddy spins up and subsequent remineralization is spatially uncoupled from the injection, a Rossby wave is a planetary wave in the classical sense and so nutrients can be uplifted continuously as they propagate westward across the ocean basin [*Siegel*, 2001]. The timescales for restoring the nutrient concentrations on the uplifted isopycnals from below the euphotic zone in the case of a Rossby wave productivity event may be different. With a Rossby wave, another possible mechanism that could help restore the nutrient concentrations below the euphotic zone back to equilibrium is that an increase in biomass in the upper waters associated with the bloom stimulated by the nutrient injection event will also decrease the availability of light at depth which could induce shoaling of the nutricline [*Letelier et al.*, 2000].

[36] During the time period of the mooring deployments (1997–1999), the T/P SSH anomalies and the 19′-hexanoyloxyfucoxanthin concentrations are negatively correlated as would be expected because low sea level anomalies imply a shallow thermocline/nitracline which would increase the nutrient flux and presumably increase phytoplankton concentrations. However, this relation does not hold throughout the HOT data record and during 1992–1995, there is a positive (but weaker) correlation with the 1996 data having no correlation and plotting as a transition period between the two phases (Figure 9). *Wilson and Adamec* [2002] found that in 66% of the global oceans the correlation is negative between SeaWiFS Chl *a* and TOPEX SSH anomaly data. However, there were significant geographic areas with positive correlations between these properties, which may be similar to the trend observed from 1992–1995 at HOT.

[37] One potential cause of a positive correlation is a decrease in the concentration of another essential nutrient that occurs concurrently with the nitrate increase. Manganese concentrations in the oligotrophic ocean typically decrease rapidly with depth in the upper 300 m [*Johnson et al.*, 1996]. Manganese concentrations are particularly low in regions of low dust input [*Klinkhammer and Bender*, 1980]. Much of the area where *Wilson and Adamec* [2002] identify positive correlations between surface chlorophyll and SSH anomaly (e.g., subpolar regions, western and central subtropical Pacific) are also areas of low dust inputs [*Duce and Tindale*, 1991]. For example, subsurface minima in manganese concentrations south of Australia in a region with strong positive correlations between chlorophyll and SSH anomaly are approximately 0.1 nM [*Sedwick et al.*, 1997], which could be sufficient to limit phytoplankton growth [*Sunda et al.*, 1981]. Iron may also have a subsurface minima, but this does not usually occur in low dust input regions and iron is not as likely to drive the positive correlations.

[38] If manganese limitation in water upwelled by Rossby waves created the positive correlation between pigments and SSH anomaly during the 1992–1995 period, then manganese concentrations would have had to be lower at that time. Unfortunately, there are no data available to resolve this question. Although it is not clear at this time why the slope of the pigment versus T/P SSH anomaly changes in 1996 at Station ALOHA, it implies that the relation between uplift of the nitracline and a biological response is complicated by other factors. The ecosystem structure, the depth of the nitracline in relation to the thermocline, the depth of the mixed layer, the light environment, the flux of trace metals, and the relative importance of nitrogen fixers all probably have an influence. To fully understand the dynamics, long-term measurements of these subsurface parameters need to be made in conjunction with the satellite measurements.

5. Conclusions

[39] The importance of Rossby waves in affecting the water column have recently been documented with the combination of moored sensors, shipboard sampling, and earth orbiting satellites. Although shipboard time series data are required to interpret the moored sensor data and to place them into a broader context, the short-term variability in nutrients and associated biological responses can best be determined by high-resolution in situ measurements. Episodic nutrient injections can promote primary productivity in the upper water column and produce shifts in phytoplankton community structure. The extent of the response will depend on the length of time that nutrients are injected into the upper waters, among other factors. Incorporating the effect of Rossby waves into oceanic models of carbon uptake and export from the euphotic zone need to be validated by long-term moored and shipboard time series sampling as the biological responses to isotherm uplift can vary spatially and temporally.

[40] **Acknowledgments.** We are grateful to the MBARI observatory support group for deployment assistance, engineering support from L. Coletti for development assistance, the Hawaii Ocean Time Series

(HOT) lab for assistance and support of the HALE ALOHA mooring deployments (T. Houlihan and L. Fujieki) and for the data provided by the HOT program (HOT program core support NSF grants to R. Lukas OCE 98-11921 and D. Karl OCE 96-17409). Thanks also to Z. Chase and two reviewers for comments on the manuscript. P. Polito was supported by FAPESP (Fundação de Amparo à Pesquisa do Estado de São Paulo, Brazil) under project 01/06921-3. Funding for the nitrate OsmoAnalyzer development and deployments was provided by the David and Lucile Packard Foundation to MBARI. Funding for the HALE ALOHA mooring and instrumentation was provided by grants from NSF (D. Karl, R. Lukas, and P. Flament, OCE 96-01850), the State of Hawaii, and NASA.

References

Andersen, R. A., R. R. Bidigare, M. D. Keller, and M. Latasa (1996), A comparison of HPLC pigment signatures and electron microscopic observations for oligotrophic waters of the North Atlantic and Pacific Oceans, *Deep Sea Res.*, *43*, 517–537.

Arimoto, R., R. A. Duce, D. L. Savoie, J. M. Prospero, R. Talbot, J. D. Cullen, U. Tomza, N. F. Lewis, and B. J. Ray (1996), Relationships among aerosol constituents from Asia and the North Pacific during PEM-West A, *J. Geophys. Res.*, *101*, 2011–2023.

Benitez-Nelson, C., K. O. Buesseler, D. M. Karl, and J. Andrews (2001), A time-series study of particulate matter export in the North Pacific subtropic gyre based on 234^{Th}:238U disequilibrium, *Deep Sea Res. Part I*, *48*, 2595–2611.

Betteridge, D., E. L. Dagless, B. Fields, and N. F. Graves (1978), A highly sensitive flow-through phototransducer for unsegmented continuous-flow analysis demonstrating high-speed spectrophotometry at the parts per 10^9 level and a new method of refractometric determinations, *Analyst*, *103*, 897–908.

Campbell, L., H. A. Nolla, and D. Vaulot (1994), The importance of *Prochlorococcus* to community structure in the central North Pacific Ocean, *Limnol. Oceanogr.*, *39*, 954–961.

Chambers, D. P., B. D. Tapley, and R. H. Stewart (1997), Long-period ocean heat storage rates and basin-scale heat fluxes from TOPEX, *J. Geophys. Res.*, *102*, 10,525–10,533.

Charria, G., F. Mélin, I. Dadou, M.-H. Radenac, and V. Garçon (2003), Rossby wave and ocean color: The cells uplifting hypothesis in the South Atlantic subtropical convergence zone, *Geophys. Res. Lett.*, *30*(3), 1125, doi:10.1029/2002GL016390.

Chelton, D. B., and M. G. Schlax (1996), Global observations of oceanic Rossby waves, *Science*, *272*, 234–238.

Cipollini, P., D. Cromwell, P. G. Challenor, and S. Raffaglio (2001), Rossby waves detected in global ocean color data, *Geophys. Res. Lett.*, *28*, 323–326.

Dandonneau, Y., A. Vega, H. Loisel, Y. D. Penhoat, and C. Menkes (2003), Oceanic Rossby waves acting as a ''Hay Rake'' for ecosystem floating by-products, *Science*, *302*, 1548–1551.

Dore, J. E., and D. M. Karl (1996), Nitrite distributions and dynamics at Station ALOHA, *Deep Sea Res. Part II*, *43*, 385–402.

Duce, R. A., and N. W. Tindale (1991), Atmospheric transport of iron and its deposition in the ocean, *Limnol. Oceanogr.*, *36*, 1715–1726.

Emerson, S., C. Stump, B. Johnson, and D. Karl (2002), In situ determination of oxygen and nitrogen dynamics in the upper ocean, *Deep Sea Res. Part I*, *49*, 941–952.

Falkowski, P. G., D. Ziemann, Z. Kolber, and P. K. Bienfang (1991), Role of eddy pumping in enhancing primary production in the ocean, *Nature*, *352*, 55–58.

Garçon, V. C., A. Oschlies, S. C. Doney, D. McGillicuddy, and J. Waniek (2001), The role of mesoscale variability on plankton dynamics in the North Atlantic, *Deep Sea Res. Part II*, *48*, 2199–2226.

Goldman, J. C. (1993), Potential role of large oceanic diatoms in new primary production, *Deep Sea Res. Part I*, *40*, 159–168.

Jannasch, H. W., K. S. Johnson, and C. M. Sakamoto (1994), Submersible, osmotically pumped analyzers for continuous determination of nitrate in situ, *Anal. Chem.*, *66*, 3352–3361.

Johnson, K. S., K. H. Coale, W. M. Berelson, and R. M. Gordon (1996), On the formation of the manganese maximum in the oxygen minimum, *Geochim. Cosmochim. Acta*, *60*, 1291–1299.

Karl, D. M. (1999), A sea of change: Biogeochemical variability in the North Pacific subtropical gyre, *Ecosystems*, *2*, 181–214.

Karl, D. M., and R. Lukas (1996), The Hawaii Ocean Time-series (HOT) program: Background, rationale, and field implementation, *Deep Sea Res. Part II*, *43*, 129–156.

Karl, D. M., and G. Tien (1997), Temporal variability in dissolved phosphorus concentrations in the subtropical North Pacific Ocean, *Mar. Chem.*, *56*, 77–96.

Karl, D. M., R. Letelier, D. V. Hebel, D. F. Bird, and C. D. Winn (1992), *Trichodesmium* blooms and new nitrogen in the north Pacific gyre, in *Marine Pelagic Cyanobacteria: Trichodesmium and Other Diazotrophs*, edited by E. J. Carpenter, D. G. Capone, and J. G. Rueter, pp. 219–237, Kluwer Acad., Norwell, Mass.

Karl, D. M., R. Letelier, D. Hebel, L. Tupas, J. Dore, J. Christian, and C. Winn (1995), Ecosystem changes in the North Pacific subtropical gyre attributed to the 1991–1992 El Niño, *Nature*, *373*, 230–234.

Karl, D., R. Letelier, L. Tupas, J. Dore, J. Christian, and D. Hebel (1997), The role of nitrogen fixation in biogeochemical cycling in the subtropical North Pacific Ocean, *Nature*, *388*, 533–538.

Karl, D. M., R. R. Bidigare, and R. M. Letelier (2001), Long-term changes in plankton community structure and productivity in the North Pacific subtropical gyre: The domain shift hypothesis, *Deep Sea Res. Part II*, *48*, 1449–1470.

Karl, D. M., R. R. Bidigare, and R. M. Letelier (2002a), Sustained and aperiodic variability in organic matter production and phototrophic microbial community structure in the North Pacific subtropical gyre, in *Phytoplankton Productivity*: *Carbon Assimilation in Marine and Freshwater Ecosystems*, edited by P. J. B. Williams, D. N. Thomas, and C. S. Reynolds, pp. 222–264, Blackwell Sci., Malden, Mass.

Karl, D. M., A. Michaels, B. Bergman, D. Capone, E. Carpenter, R. Letelier, F. Lipschultz, H. Paerl, D. Sigman, and L. Stal (2002b), Dinitrogen fixation in the world's oceans, *Biogeochemistry*, *57/58*, 47–98.

Karl, D. M., et al. (2003a), Temporal studies of biogeochemical processes determined from ocean time-series observations during the JGOFS era, in *Ocean Biogeochemistry*: *The Role of the Ocean Carbon Cyclein Global Change*, edited by M. J. R. Fasham, pp. 239–267, Springer-Verlag, New York.

Karl, D. M., E. A. Laws, P. Morris, P. J. LeB. Williams, and S. Emerson (2003b), Metabolic balance of the open sea, *Nature*, *426*, 32.

Klinkhammer, G. P., and M. L. Bender (1980), The distribution of manganese in the Pacific Ocean, *Earth Planet. Sci. Lett.*, *46*, 361–384.

Letelier, R. M., D. M. Karl, M. R. Abbott, P. Flament, M. Freilich, R. Lukas, and T. Strub (2000), Role of late winter mesoscale events in the biogeochemical variability of the upper water column of the North Pacific subtropical gyre, *J. Geophys. Res.*, *105*, 28,723–28,739.

Letelier, R. M., D. M. Karl, M. R. Abbott, and R. R. Bidigare (2004), Light driven seasonal patterns of chlorophyll and nitrate in the lower euphotic zone of the North Pacific Subtropical Gyre, *Limnol. Oceanogr.*, *49*, 508–519.

Lewis, M. R. (2002), Variability of plankton and plankton processes on the mesoscale, in *Phytoplankton Productivity*: *Carbon Assimilation in Marine and Freshwater Ecosystems*, edited by P. J. B. Williams, D. N. Thomas, and C. S. Reynolds, pp. 141–155, Blackwell Sci., Malden, Mass.

Lewis, M. R., W. G. Harrison, N. S. Oakey, D. Herbert, and T. Platt (1986), Vertical nitrate fluxes in the oligotrophic ocean, *Science*, *234*, 870–873.

Mahadevan, A., and D. Archer (2000), Modeling the impact of fronts and mesoscale circulation on the nutrient supply and biogeochemistry of the upper ocean, *J. Geophys. Res.*, *105*, 1209–1225.

Martin, A. P., K. J. Richards, and M. J. R. Fasham (2001), Phytoplankton production and community structure in an unstable frontal region, *J. Mar. Syst.*, *28*, 65–89.

McGillicuddy, D. J., Jr., and A. R. Robinson (1997), Eddy-induced nutrient supply and new production in the Sargasso Sea, *Deep Sea Res. Part I*, *44*, 1427–1450.

McGillicuddy, D. J., Jr., A. R. Robinson, D. A. Siegel, H. W. Jannasch, R. Johnson, T. D. Dickey, J. McNeil, A. F. Michaels, and A. H. Knap (1998), Influence of mesoscale eddies on new production in the Sargasso Sea, *Nature*, *394*, 263–266.

McGillicuddy, D. J., Jr., R. Johnson, D. A. Siegel, A. F. Michaels, N. R. Bates, and A. H. Knap (1999), Mesoscale variations of biogeochemical properties in the Sargasso Sea, *J. Geophys. Res.*, *104*, 13,381–13,394.

McGillicuddy, D. J., Jr., L. A. Anderson, S. C. Doney, and M. E. Maltrud (2003), Eddy-driven sources and sinks of nutrients in the upper ocean: Results from a 0.1° resolution model of the North Atlantic, *Global Biogeochem. Cycles*, *17*(2), 1035, doi:10.1029/2002GB001987.

McNeil, J. D., H. W. Jannasch, T. Dickey, D. McGillicuddy, M. Brzezinski, and C. M. Sakamoto (1999), New chemical, bio-optical and physical observations of upper ocean response to the passage of a mesoscale eddy off Bermuda, *J. Geophys. Res.*, *104*, 15,537–15,548.

Michaels, A. F., D. Olson, J. L. Sarmiento, J. W. Ammerman, K. Fanning, R. Jahnke, A. H. Knap, F. Lipschultz, and J. M. Prospero (1996), Inputs, losses and transformations of nitrogen and phosphorus in the pelagic North Atlantic Ocean, *Biogeochemistry*, *35*, 181–226.

Moore, L. R., A. F. Post, G. Rocap, and S. W. Chisholm (2002), Utilization of different nitrogen sources by marine cyanobacteria, *Limnol. Oceanogr.*, *47*, 989–996.

Planas, D., S. Agusti, C. M. Duarte, T. C. Granata, and M. Merino (1999), Nitrate uptake and diffusive nitrate supply in the central Atlantic, *Limnol. Oceanogr.*, *44*, 116–126.

Polito, P. S., and W. T. Liu (2003), Global characterization of Rossby waves at several spectral bands, *J. Geophys. Res.*, *108*(C1), 3018, doi:10.1029/2000JC000607.

Polito, P. S., O. T. Sato, and W. T. Liu (2000), Characterization and validation of the heat storage variability from TOPEX/Poseidon at four oceanographic sites, *J. Geophys. Res.*, *105*, 16,911–16,921.

Prospero, J. M., and D. L. Savoie (1989), Effect of continental sources on nitrate concentrations over the Pacific Ocean, *Nature*, *339*, 687–689.

Scharek, R., M. Latasa, D. M. Karl, and R. R. Bidigare (1999), Temporal variations in diatom abundance and downward vertical flux in the oligotrophic North Pacific gyre, *Deep Sea Res. Part I*, *46*, 1051–1075.

Sedwick, P. N., P. R. Edwards, D. J. Mackey, F. B. Griffiths, and J. S. Parslow (1997), Iron and manganese in surface waters of the Australian subantarctic region, *Deep Sea Res. Part I*, *44*, 1239–1253.

Siegel, D. A. (2001), Oceanography: The Rossby rototiller, *Nature*, *409*, 576–577.

Siegel, D. A., D. J. McGillicuddy Jr., and E. A. Fields (1999), Mesoscale eddies, satellite altimetry, and new production in the Sargasso Sea, *J. Geophys. Res.*, *104*, 13,359–13,379.

Sun, J., M. Zhang, and T. Liu (2001), Spatial and temporal characteristics of dust storms in China and its surrounding regions, 1960–1999: Relations to source area and climate, *J. Geophys. Res.*, *106*, 10,325–10,333.

Sunda, W. G., R. T. Barber, and S. A. Huntsman (1981), Phytoplankton growth in nutrient rich seawater: Importance of copper-manganese cellular interactions, *J. Mar. Res.*, *49*, 567–586.

Uz, B. M., J. A. Yoder, and V. Osychny (2001), Pumping of nutrients to ocean surface waters by the action of propagating planetary waves, *Nature*, *409*, 597–600.

Villareal, T. A., and E. J. Carpenter (2003), Buoyancy regulation and the potential for vertical migration in the oceanic cyanobacterium *Trichodesmium*, *Microbial Ecol.*, *45*, 1–10.

Wilson, C., and D. Adamec (2002), A global view of bio-physical coupling from SeaWiFS and TOPEX satellite data, 1997–2001, *Geophys. Res. Lett.*, *29*(8), 1257, doi:10.1029/2001GL014063.

Zehr, J. P., J. B. Waterbury, P. J. Turner, J. P. Montoya, E. Omoregie, G. F. Steward, A. Hansen, and D. M. Karl (2001), Unicellular cyanobacteria fix N_2 in the subtropical North Pacific Ocean, *Nature*, *412*, 635–638.

R. R. Bidigare and D. M. Karl, Department of Oceanography, University of Hawaii, 1000 Pope Road, Marine Sciences Building, Honolulu, HI 96822, USA.

H. W. Jannasch, K. S. Johnson, J. P. Ryan, C. M. Sakamoto, and P. M. Walz, Monterey Bay Aquarium Research Institute, 7700 Sandholdt Road, Moss Landing, CA 95039, USA. (saca@mbari.org)

R. M. Letelier, College of Oceanic and Atmospheric Sciences, Oregon State University, 140 Burt Hall, Corvallis, OR 97331-1301, USA.

P. S. Polito, Instituto Nacional de Pesquisas Espaciais, São José dos Campos,191, São Paulo 05508-120, Brazil.